Excitation of the $^{119}Te^{m}$, $^{121}Te^{m}$, $^{123}Te^{m}$, $^{127}Te^{m}$, and $^{129}Te^{m}$ isomers in (γ,n) reactions from 10 to 22 MeV

V. M. Mazur, D. M. Symochko,* Z. M. Bigan, and T. V. Poltorzhytska
Institute of Electron Physics of NAS of Ukraine, Uzhhorod, Ukraine
(Received 11 August 2012; revised manuscript received 25 December 2012; published 4 April 2013)

Isomeric yield ratios for the ^{119}Te, ^{121}Te, ^{123}Te, ^{127}Te, and ^{129}Te nuclei were obtained in (γ,n) reactions with bremsstrahlung endpoint energies ranging from 10 to 22 MeV in steps of 0.5 MeV. Experimental isomeric ratios were used to calculate the cross sections of $(\gamma,n)^m$ reactions, which were further compared with TALYS-1.4 calculations.

DOI: 10.1103/PhysRevC.87.044604 PACS number(s): 25.20.Dc, 23.35.+g, 27.60.+j

I. INTRODUCTION

γ-ray beams are an accurate tool for investigating different processes in nuclear physics and astrophysics. Photons with energies of tens MeV bring relatively small changes to nuclei (comparing with charged and massive particles) and due to the pure electromagnetic character of photonuclear reactions may be used to obtain information on nucleon-nucleon interactions [1,2], collective motions of the nuclear matter [giant dipole resonance (GDR), pygmy dipole resonance, etc.)] [3], mechanisms of the particular nuclear-state excitation [4,5], etc.

Photonuclear reactions are also important for understanding the processes of element creation in a stellar environment. In cosmic nucleosynthesis, nuclei heavier than iron are mainly produced via the chain of neutron capture reactions named *r* and *s* astrophysical processes. However, there are few dozen neutron-deficient stable nuclides screened by stable isobars from neutron capture [6]. They are called *p*-nuclei and are synthesized mainly through the chain of photonuclear reactions on *r*- or *s*-seed nuclei [7,8]. ^{120}Te is one of these *p*-process nuclei and the reaction ^{120}Te$(\gamma,n)^{119}$Te partly determines the cross section of its photodisintegration. Moreover, in view of the fact that ^{120}Te is produced by photodisintegration of the *s*-only nucleus ^{122}Te followed by that of ^{121}Te, cross sections of ^{122}Te$(\gamma,n)^{121}$Te may be treated as a part of production cross section of the *p*-nucleus.

A database that includes exact values for thousands of reaction cross sections is required in order to determine *p*-abundances. As experimental information on reactions involved in the *p*-process is very scarce [9]; reaction rates based on calculations within the Hauser-Feshbach formalism [10] are used for modeling of the *p*-process flow.

One of the methods for checking the conformity of statistical model based on compound nucleus assumption involves the comparison of its results with experimental data on isomeric-state population—isomeric ratios and cross sections. The modeling of partial reactions is not a trivial task because, in addition to the determination of total cross sections, it demands accurate treatment of the processes taking place in the residual nucleus (γ cascade, particle emission).

The isomeric ratios and cross sections of $(\gamma,n)^m$ reactions on Te isotopes in the GDR energy region were previously insufficiently studied. There are only two published works [11,12] that contain complex studies of Te isomeric-yield ratios, which were, however, measured for only particular energies up to $E_{\gamma max} = 25$ MeV. At the same time, Te isotopes are remarkable because they allowed the investigation of the evolution of isomeric ratios with the change of neutron subshell population through a wide mass range ($A = 119$–130). All tellurium isomers are characterized by spin-parity $J^{\pi} = 11/2^{-}$ and are formed by the $1h_{11/2}$ subshell. Ground states of ^{119}Te, ^{121}Te, and ^{123}Te, isotopes are formed by $3s_{1/2}$ subshell, while in ^{127}Te, ^{129}Te they are formed by $2d_{3/2}$.

Therefore, the objective of this study is to present the following:

(i) Measurements of isomeric-yield ratios' $d = Y_m/Y_g$ dependence on bremsstrahlung endpoint energy in the (γ,n) reactions on ^{119}Te, ^{121}Te, ^{123}Te, ^{127}Te, and ^{129}Te isotopes for the energy range $E_{\gamma max} = 10$–22 MeV (Secs. II and III).

(ii) Determination of ^{124}Te$(\gamma,n)^{123}$Te^m, ^{128}Te$(\gamma,n)^{127}$Te^m, and ^{130}Te$(\gamma,n)^{129}$Te^m reaction cross sections in the energy region of the giant dipole resonance (Secs. II and III).

(iii) Calculation of Te isotopes' isomeric-state population cross sections with the TALYS-1.4 code [13] and further comparison with the obtained experimental data (Sec. IV).

II. EXPERIMENT

A. Targets and irradiation

Samples were irradiated with a bremsstrahlung beam from electron accelerator Microtron M-30 (Institute of Electron Physics of National Academy of Sciences of Ukraine) [14] within the 10–18 MeV endpoint-energy range in $\Delta E = 0.5$ MeV steps. The electron beam extracted from the accelerator was converted into bremsstrahlung with a 0.5-mm-thick tantalum radiator. The energy of the electron beam can be tuned using two methods: (i) in the wide energy range—by replacing the wave guide insets, i.e., by varying the number of electron beam orbits, and (ii) within the energy limits of single inset—by varying the magnetic field of the microtron. The intensity of the magnetic field was measured by the NMR method

*Present address: Technische Universität Darmstadt, Institut für Kernphysik, Schlossgartenstraße 9, 64289 Darmstadt, Germany.

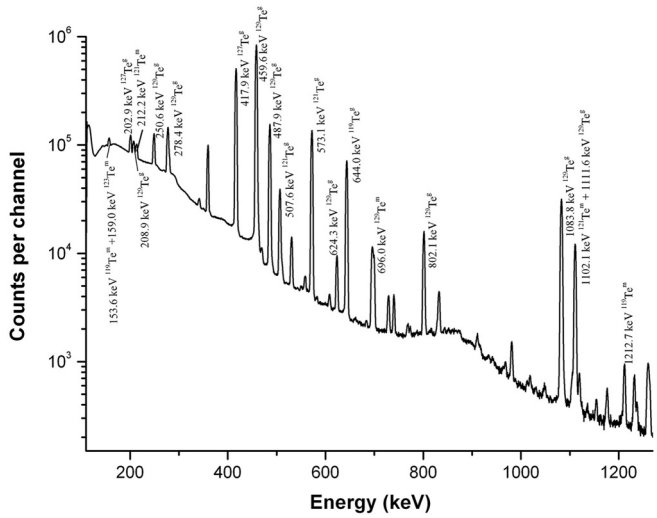

FIG. 1. Typical γ-ray spectrum from measuring the activated tellurium sample using a HPGe detector. Counting time was 24 hours, $E_{\gamma\max} = 15$ MeV.

and it allowed us to achieve less than 50 keV uncertainties in the electron-beam-energy spread determination. The mean current (5 μA) of beam electrons was controlled with a secondary-emission monitor with the 1.2 s time step. For the energies 20–22 MeV the bremsstrahlung beam from the betatron B25/30 of Uzhhorod National University was used; tellurium targets were placed on the beam axis at a distance of 30 cm from the tantalum radiator. Targets were made of glass-like TeO_2 of natural isotopic composition (99.99% chemical purity) in the form of disks (25 mm diameter, 2.5 mm thick).

B. Measurements

The activation technique was used in the experiment. Specifically, induced activity in the targets was measured offline after irradiation and cooling periods. Since lifetimes of investigated states are relatively long it allowed us to carry out the measurements in good background conditions and observe even low-intensity γ-ray lines. Isomeric states and unstable ground states were produced during the same irradiation session, thus the isomeric ratios were determined with high precision.

Following the irradiations and cooling period, the residual activity in the samples was measured in a low-background environment with spectroscopic system consisting of a 175 cm^3 HPGe detector and a multichannel analyzer manufactured by "EG&G ORTEC". The detector was screened from background radiation by the combined Pb-Cd-Cu shield. The energy resolution of the detector was 2 keV for ^{60}Co γ rays. Efficiency calibrations were done with the reference radioactive sources: ^{60}Co, ^{137}Cs, ^{152}Eu (standard uncertainty $\approx$2%).

To extract optimal amount of data from the decay of the residual nuclei the measurement process was organized as described below. Irradiation periods varied from 2 hours for near-threshold energies to 20 minutes for energies greater than 15 MeV. After irradiation and 1 to 2 hours cooling (needed to reduce the dead time of the detector) the decay of the ^{129}Te^g ground state was measured. γ spectra obtained during next 24 hours were used to obtain data on the decay of the ^{119}Te^m, ^{127}Te^m, and ^{129}Te^m states. Measurements of long-lived reaction products were performed during 1–3 days after 7–20 days of cooling.

Part of the typical spectrum from an irradiated tellurium sample is shown in Fig. 1. We used spectroscopic data for the investigated nuclei from Refs. [15–19] (Table I).

Table I gives the neutron separation energy S_n from the initial nucleus, the spin parity J^π of the levels, the half-lives $T_{1/2}$ of the levels, the energies E_m of the isomeric levels, the energies E_γ of the analytical γ-ray lines, the intensity α of the analytical γ-ray lines, and the "isomer-to-ground" branching ratio p.

III. RESULTS

Direct outcome of the experiments, which were performed with bremsstrahlung beams, includes the yields Y, which are connected with the cross sections σ through the integral equation

$$Y(E_m) = k \int_{E_{\rm th}}^{E_{\gamma\max}} \sigma(E)\Phi(E, E_{\gamma\max})dE, \qquad (1)$$

TABLE I. Spectroscopic data for investigated nuclei.

	S_n (MeV)	J^π	$T_{1/2}$	E_m (keV)	E_γ (keV)	α (%)	p (%)
^{119}Te^m		$11/2^-$	4.70 days	261.0	1212.7	66.1	<0.008
^{119}Te^g	10.296	$1/2^+$	16.05 hours	0.0	644.0	84.1	
^{121}Te^m		$11/2^-$	164.2 days	294.0	212.2	81.5	88.6
^{121}Te^g	9.834	$1/2^+$	19.17 days	0.0	573.1	80.4	
^{123}Te^m		$11/2^-$	119.2 days	247.5	159.0	84.0	100.0
^{123}Te^g	9.424	$1/2^+$	stable	0.0			
^{127}Te^m		$11/2^-$	106.1 days	88.3	88.3	0.084	97.6
^{127}Te^g	8.775	$3/2^+$	9.35 hours	0.0	417.9	0.99	
^{129}Te^m		$11/2^-$	33.6 days	105.5	696.0	3.19	63.0
^{129}Te^g	8.419	$3/2^+$	69.6 min	0.0	459.6	7.7	

where $\Phi(E, E_{\gamma max})$ is the bremsstrahlung spectrum, E_{th} is the reaction threshold energy, $E_{\gamma max}$ is the bremsstrahlung endpoint energy, and k is the normalization coefficient. In the general case, the isomeric-yield ratios d are determined as [20]

$$d(E_{\gamma max}) = \frac{Y_m}{Y_n} = \left\{ c\frac{\lambda_g}{\lambda_m}\frac{f_m(t)}{f_g(t)}\left(\frac{\varphi_m}{\varphi_g}\frac{N_g}{N_m} - p\frac{\lambda_g}{\lambda_g - \lambda_m}\right) + p\frac{\lambda_m}{\lambda_g - \lambda_m}\right\}^{-1}, \quad (2)$$

where N_m and N_g are the counts in photopeaks associated with isomer and ground state decay, respectively, φ_m and φ_g are the coefficients which include the detector efficiency ϵ, self-absorption μ in the targets, and the γ-ray line intensity α, p is the branching ratio, c is the correction factor for detector "dead time" and pulse overlapping, and the f_m and f_g time factors are expressed in following way:

$$f_m = [1 - \exp(-\lambda_m t_{irr})]\exp(-\lambda_m t_{cool})[1 - \exp(-\lambda_m t_{meas})],$$
$$f_g = [1 - \exp(-\lambda_g t_{irr})]\exp(-\lambda_g t_{cool})[1 - \exp(-\lambda_g t_{meas})],$$

where λ_m and λ_g denote the decay constants of the isomeric and ground states, and t_{irr}, t_{cool}, and t_{meas} are the intervals of irradiation, cooling, and measurements.

However, for the tellurium isotopes in which the half-lives of the ground states are significantly smaller than those for the isomeric (^{127}Te, ^{129}Te) it was reasonable to separate the measurements in time in order to separate the state decay and treat their yields as independent values. In these cases isomeric ratios were obtained with the expression

$$d(E_{\gamma max}) = Y_m/Y_g = \frac{N_m}{N_g}\frac{c_m}{c_g}\frac{\lambda_m}{\lambda_g}\frac{\varphi_g}{\varphi_m}\frac{f_g(t)}{f_m(t)}, \quad (3)$$

Naturally, measurement (t^m_{meas},t^g_{meas}) and cooling (t^m_{cool},t^g_{cool}) intervals were different for different states. Ground-state yields were measured immediately after the irradiation. Since $T^m_{1/2} \gg T^g_{1/2}$ the contribution of isomers decay in them was negligible. The error caused by the procedure does not exceed 0.5%.

A. ^{128}Te(γ,n)^{127} Te^{m,g}

We used the analytical γ-ray line from the ground state decay 417.9 keV ($\alpha = 0.993$) twice because of the low intensity of the $^{127}Te^m$ decay γ and rather high "isomer-to-ground" branching ratio. Following irradiation and 2 to 3 hours of cooling, the yield of the $^{127}Te^g$ state was measured. The next measurement was carried out after 7–10 days when the initial number of nuclei resulted from the ^{128}Te(γ,n)$^{127}Te^g$ reaction decreased 10^5–10^6 times and the population of the ground state was determined only by the decay of the isomer, since the system came to the equilibrium condition $\lambda_g N_g = \lambda_m N_m$. Thus, the ground-state decay with the half-life of the isomer and the 417.9 keV line was used for indicating the decay of the isomeric state during this counting interval. Consequently, Eq. (3) transforms into the following expression:

$$d(E_{\gamma max}) = Y_m/Y_g = \frac{N_m}{N_g}\frac{c_m}{c_g}\frac{\lambda_m}{\lambda_g}\frac{1}{p}\frac{f_g(t)}{f_m(t)}. \quad (4)$$

B. ^{124}Te(γ,n) ^{123}Te^{m,g}

The ground state $^{123}Te^g$ is stable and it is impossible to estimate its population in the conditions of our experiment. However, considering the data on total cross section of (γ,n) reactions on tellurium isotopes [21] it can be seen that the variations of the parameters are very small from isotope to isotope. It allowed us to use the simultaneously measured total yield $Y_n = Y_g + Y_m$ of the reaction ^{122}Te(γ,n)$^{122}Te^{m,g}$ to estimate the isomeric ratio in the reaction ^{124}Te(γ,n)$^{123}Te^{m,g}$. Although the cross section of the $(\gamma, \gamma)^m$ reaction is two orders of magnitude lower than those of the reactions $(\gamma,n)^m$ and the abundance of ^{123}Te in natural isotopic composition is only 0.87%, we made the correction for the ^{123}Te(γ, γ)$^{123}Te^m$ reaction contribution to the population of the $^{123}Te^m$ state as it can be noteworthily important in the near-threshold region.

Obtained with the above-mentioned procedures, experimental isomeric-yield ratios $d = f(E_{\gamma max})$ for the ^{120}Te(γ,n)$^{119}Te^{m,g}$, ^{122}Te(γ,n)$^{121}Te^{m,g}$, ^{124}Te(γ,n)$^{123}Te^{m,g}$, ^{128}Te(γ,n)$^{127}Te^{m,g}$, and ^{130}Te(γ,n)$^{129}Te^{m,g}$ reactions with standard errors determined from a series of measurements are shown as dots in Fig. 2. Essentially, dependencies $d = f(E_{\gamma max})$ grow from the $(\gamma,n)^m$ reactions thresholds for all presented cases and reach the plateau within a 20–22 MeV energy range. Statistical error of every single measurement was 2% to 3% near the threshold and decreased to 0.2% to 0.4% for the energies greater than 14.5 MeV. Magnitudes of main sources of systematic uncertainties were in the following limits: sample mass determination $\leqslant$0.5%, detector efficiency was 2%, branching ratios was $\leqslant$1%, product half-lives were $\leqslant$1%, γ-ray-line intensities were $\leqslant$1%.

The solid lines in Fig. 2 resulted from approximating the experimental isomeric ratios with Boltzmann curves:

$$y = A + (B - A)/\{1 + \exp[(E - E_0)/\Delta E]\}, \quad (5)$$

TABLE II. Boltzmann curve parameters values.

Isotope	A	B	E_0 (MeV)	ΔE (MeV)
^{119}Te	0.184(3)	− 0.064 54(20)	14.03(37)	2.21(2)
^{121}Te	0.224(10)	− 0.1135(40)	12.60(48)	2.07(3)
^{123}Te	0.228(4)	− 0.1513(30)	12.03(31)	2.71(5)
^{127}Te	0.315(20)	− 0.0496(20)	13.92(19)	1.99(20)
^{129}Te	0.440(6)	− 0.053(6)	14.13(6)	1.97(8)

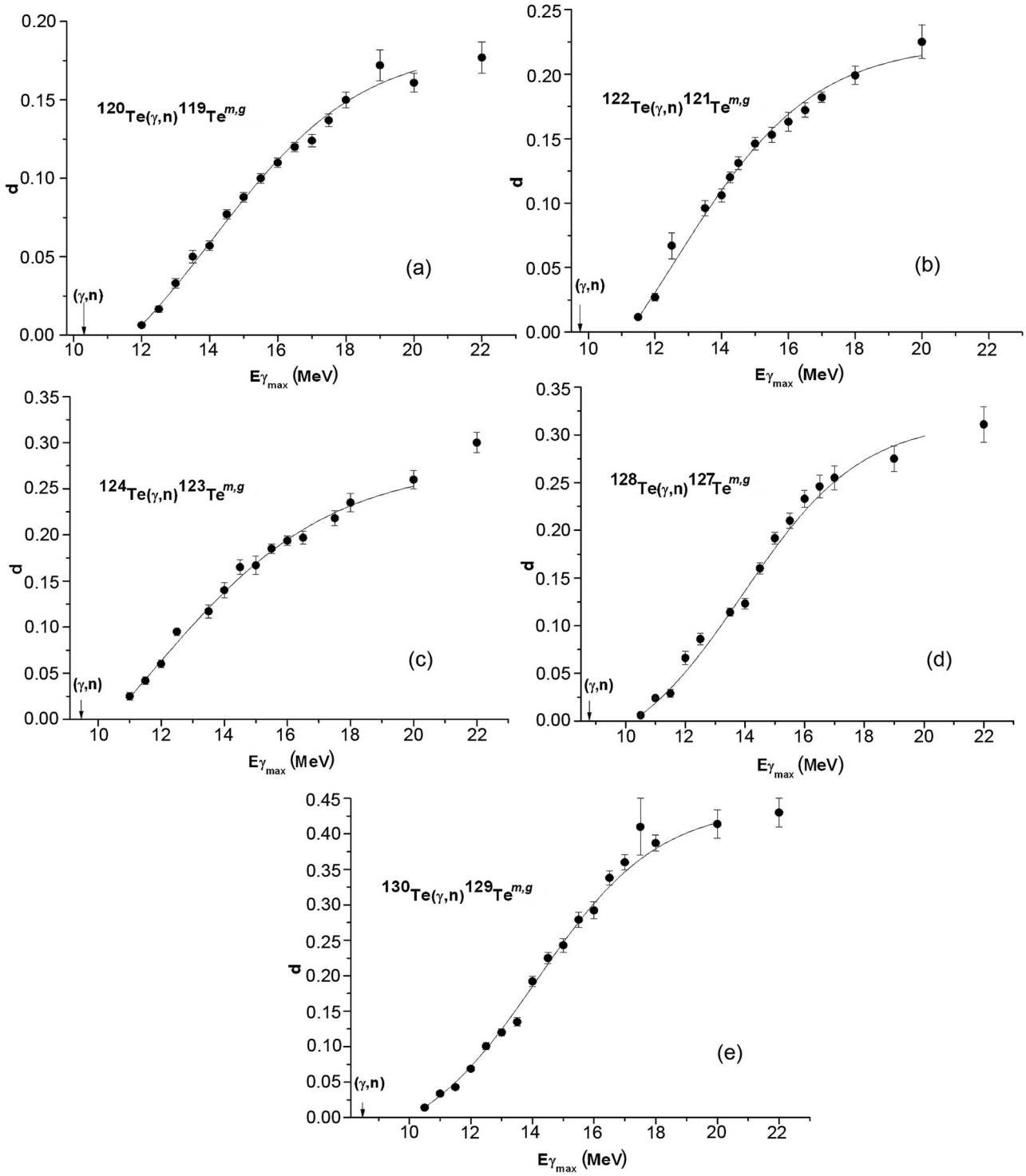

FIG. 2. Experimental isomeric-yield ratios for the ^{120}Te$(\gamma,n)^{119}$Te^{m,g}, ^{122}Te$(\gamma,n)^{121}$Te^{m,g}, ^{124}Te$(\gamma,n)^{123}$Te^{m,g}, ^{128}Te$(\gamma,n)^{127}$Te^{m,g}, and ^{130}Te$(\gamma,n)^{129}$Te^{m,g} reactions. Dots are experimental values and solid line is an approximation of the experimental results.

where A, B, E_0, and ΔE are parameters. The approximation was carried out with a least-squares method within the range from reaction thresholds up to 20 MeV. The parameter values are presented in Table II. We would like to point that extrapolation of our data to higher energies leads to excellent agreement with the isomeric ratios measured at 25 MeV endpoint energy published in Ref. [11].

Experimental dependence of the isomeric-yield ratios on the bremsstrahlung endpoint energy $d = f(E_{\gamma\max})$ allows us to calculate the experimental isomeric-state population cross

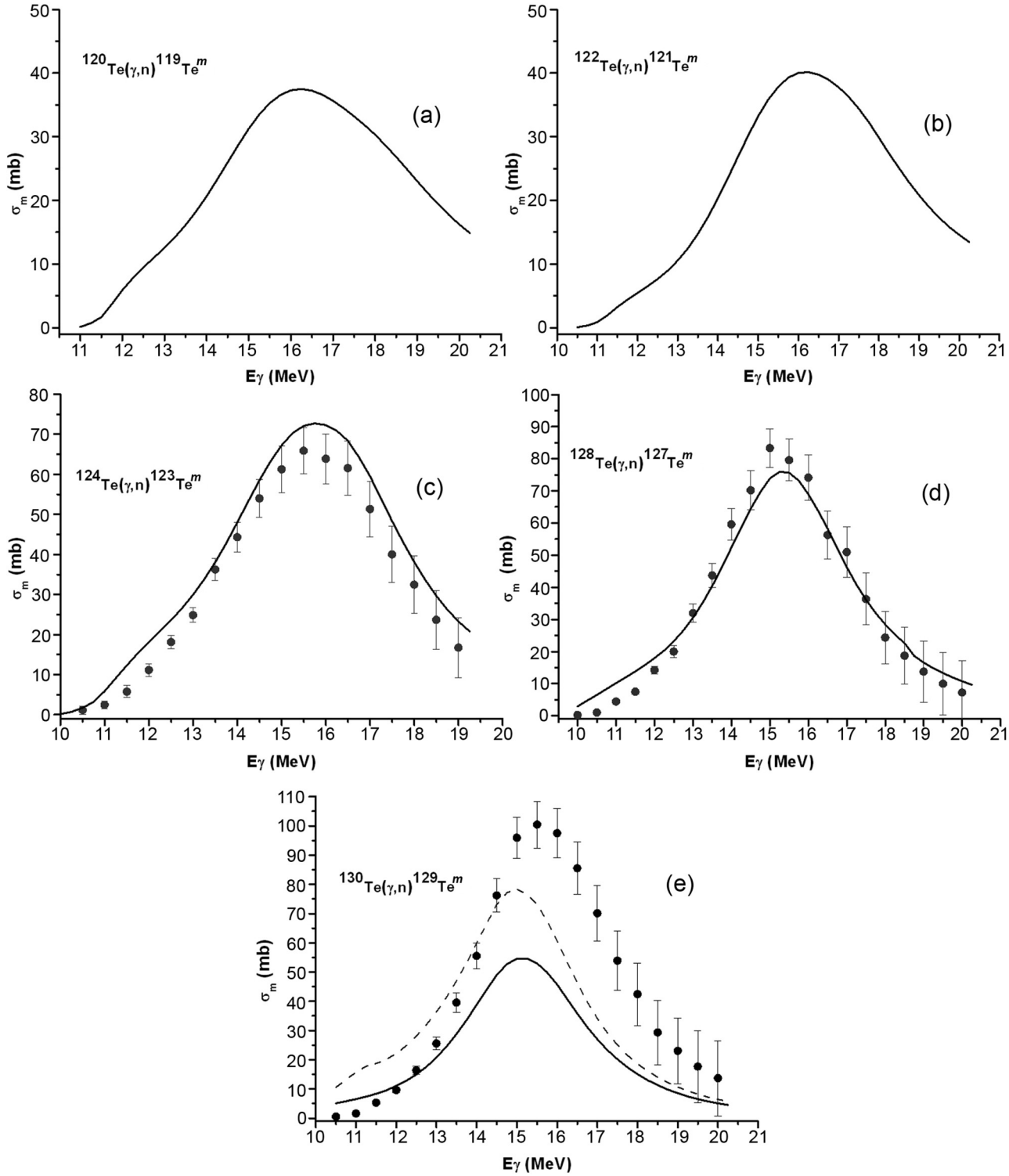

FIG. 3. Cross sections of $^{120}Te(\gamma,n)^{119}Te^{m}$, $^{122}Te(\gamma,n)^{121}Te^{m}$, $^{124}Te(\gamma,n)^{123}Te^{m}$, $^{128}Te(\gamma,n)^{127}Te^{m}$, and $^{130}Te(\gamma,n)^{129}Te^{m}$. Dots are experimental values, solid lines show TALYS-1.4 calculations with RIPL-3 standard level structure, dashed line shows a TALYS-1.4 calculation with a modified level structure.

sections σ_m using known total (γ,n) reaction cross sections [21]. The calculation was carried out with the reverse matrix method [22]. The yield curves were smoothed before used as an input for the calculations. Uncertainties of the calculated cross sections were determined according to the procedure described in Ref. [22]. It also has to be taken into account that systematic uncertainty caused by normalization to the total cross section from Ref. [21] is near 5%.

TABLE III. Lorentz curves parameters values.

	σ_{tot} Ref. [21]			σ_m		
	^{124}Te	^{128}Te	^{130}Te	^{124}Te	^{128}Te	^{130}Te
σ_0 (mb)	281(15)	304(15)	318(16)	68.6(26)	80.2(10)	107(5)
Γ_0 (MeV)	5.5(2)	5.4(2)	5.1(2)	4.2(2)	4.0(1)	3.4(2)
E_0 (MeV)	15.2(1)	15.1(1)	15.1(2)	15.5(1)	15.4(1)	15.1(1)

Obtained cross sections of isomer populations in the ^{124}Te$(\gamma,n)^{123}$Te^m, ^{128}Te$(\gamma,n)^{127}$Te^m, and ^{130}Te$(\gamma,n)^{129}$Te^m reactions are presented as dots in the Fig. 3. We are not presenting results of calculations for ^{120}Te$(\gamma,n)^{119}$Te^m and ^{122}Te$(\gamma,n)^{121}$Te^m reactions because there are no published experimental data on total (γ,n) cross sections for these isotopes. The parameters of the Lorenz curves fit to the obtained isomeric cross sections together with the literature parameters of total cross sections σ_{tot} taken from Ref. [21] are shown in Table III.

Figures 2 and 3 reveal that isomeric-yield ratios and cross sections are increasing with growth of isotope mass from $A = 119$ to $A = 129$. It correlates with the population of the outer subshell $1h_{11/2}$, which starts to fill from ^{122}Te and reaches eight neutrons in ^{130}Te.

IV. MODEL CALCULATIONS

In order to compare experimental and theoretical data on isomeric excitation we calculated the reaction cross sections with the help of the TALYS-1.4 code.

The following scheme was used in calculations: A dipole monochromatic γ ray with $E\gamma$ energy interacts with a nuclear target (Z_i, N_i) and the compound state (J_c, π_c) is formed with excitation energy E_c equal to the energy of incident γ ray. The total photoabsorption cross section σ_{tot} is calculated with the use of experimental GDR parameters (if available) or from semiempirical systematics.

Both statistical and pre-equilibrium mechanisms contribute to the decay process of the residual nuclei. The main contribution in the investigated energy region belongs to the Hauser-Feshbach statistical mechanism. But with the increase of energy, the part of the pre-equilibrium processes simulated with the exciton model [23–25] becomes more significant. After γ-ray absorption the particle-hole pair (exciton) is created. The system evolves through the steps and the number of excitons for each is increased by one. Particle emission is possible from every stage of the process. After six steps the process is no longer treated as pre-equilibrium and further reaction flow is simulated with a statistical model.

The calculated contribution of pre-equilibrium processes to the total photoneutron reaction cross section on Te isotopes for 12, 16, and 18 MeV energies are showed in Table IV. Calculations show that statistical mechanisms dominate for the GDR region and its contribution to the total (γ,n) cross sections even for higher energies is more than 80%.

After neutron emission the population of the particular residual nucleus levels is calculated using the transmission coefficients T_l obtained from the optical model [26]. The RIPL-3 database [27] was used to obtain information on the first 80 discreet levels. At higher energies, the excited-state spectrum was treated as continuous. It was described by the level density $\rho(E, J, \pi)$ and divided into 40 equidistant energy bins. If the nucleus decays to continuous spectrum bins, then the effective transmission coefficient T_l^{eff} is used. For simulation of the continuous spectra we used the back-shifted Fermi-gas model [28].

The calculated cross sections are plotted in Fig. 3 with solid lines. Calculated values are significantly consistent with experimental data for ^{124m}Te and ^{127m}Te, but at the same time we may see very poor agreement in the case of ^{129m}Te. Notable disagreement (more than 50% at the maximum) for the reaction ^{130}Te$(\gamma,n)^{129}$Te^m stimulated additional research. We found that the information on discreet levels for the ^{129}Te used in the RIPL-3 database originated from the Evaluated Nuclear Structure Data File (ENSDF) [19] which (in case of $A = 129$) has not been updated since 1996. However, the detailed study of ^{129}Te structure was published in 2003 [29]. This paper introduces the 1221 keV level with $J^\pi = 5/2^-$ which may be the key to understanding the strong population of the ^{129m}Te isomer. This level effectively accumulate the intensity from higher-lying $3/2^-$ states, which can be easily excited in (γ,n) reactions. The substantial part of neutrons will be emitted with $L = 0$ moments after the decay of the 1^- state of the giant dipole resonance via the photoneutron channel and it leads to the direct excitation of $3/2^-$ levels in the residual nuclei. About 42% of the intensity feeding the isomers goes through this level. Furthermore, the $7/2^-$ state at 1162 keV plays an important role in redirecting about 25% of the intensity to the isomer. Similar mechanisms of the isomer population were found in the other Te isotopes [29,30].

We modified the level-structure file according to the information published in Ref. [29] and performed additional calculations (shown as solid lines in Fig. 3). We can see that calculations with updated data lead to significantly better agreement with experimental cross sections.

TABLE IV. Calculated contribution of pre-equilibrium processes to $(\gamma,n)^m$ reaction cross section.

Isotope	12 MeV	16 MeV	18 MeV
^{124}Te	0.46%	5.7%	9.4%
^{128}Te	0.99%	7.4%	11.3%
^{130}Te	1.3%	8.5%	12.5%

Here we should note that such calculations are highly sensitive to the information about nuclear structure. For example, changing the J value for a single level of ^{129}Te (level energy 455 keV, possible spin-parity values $7/2^+$, $9/2^+$) resulted in about 10% change for the ^{130}Te$(\gamma,n)^{129}$Te^m reaction cross section. Therefore, one can hardly rely on the model calculations for obtaining populations of particular nuclear levels (e.g., isomers) if data on at least low-energy-level J^π values and the branching ratio is not complete.

In the statistical model, because of averaging of the large number of overlapping states, we can neglect the matrix-element features that describe the decay of particular states. It results in a similarity of transition-matrix elements, i.e., the final levels for the decay of a particular state are equal. Thus, the probability of a particular transition is proportional to the final density of states and depends on the transition's multipolarity.

In TALYS-1.4, calculations of the γ-transition probabilities are derived from the γ-ray strength functions. For $E1$ transitions the generalized Lorentzian form of Kopecky and Uhl [31] was used, while for the transitions of other multipolarities were standard Lorentzian (Brink-Axel form) [32,33]. It should be noted that $E1$ transitions are dominating in calculated γ-cascade (90%) with a very little admixture of $E2$ and $M1$ radiation.

The situation is different in the low-energy part of the spectra where the microscopic calculations of level structure can be performed. In Ref, [29] it was mentioned that all the states in ^{129}Te of negative parity lower than 1100 keV are only weakly populated in (d, p) reactions which may serve as a sign of their complicated structure [34,35]. The interacting boson-fermion model (IBFM) describes states $3/2^-$ and $5/2^-$ of ^{129}Te as a mixture of the $1h_{11/2}$ neutron wave function as a main part with a small $3p$ component, coupled to the first 4^+ state of the core [30,36]. The IBFM calculations reproduce well the energy of the states and confirm the enhanced $E2$ transitions between the levels of negative parity due to the admixed quadrupole phonons.

According to the analysis of the γ transitions between low-energy levels [9] we can see that the part of the $E1$ transitions is extremely low. States of positive parity decay by $M1$ and $E2$ transitions and do not populate levels of negative parity. Their decay path leads to final level $J^\pi = 3/2^+$ and practically does not contribute to the population of the $J^\pi = 11/2^-$ isomer. As mentioned above, the enhanced $E2$ transitions are observed between negative-parity states. Therefore the transitions probabilities are mainly defined by their microscopic nature. It is highly possible that the same is true for higher energies described in the calculations as continuous spectra.

As mentioned before, the main part of the Te isomer excitation cross section belongs to the statistical mechanism. But the growth of the isomeric population and the cross section of the $(\gamma,n)^m$ reactions with the increase of isotope mass cannot be explained in the framework of the statistical model. It would be natural to suggest that the increasing contribution of pre-equilibrium processes can be responsible for that, but calculations showed that their share is too low to explain this effect. Experimental data on the nuclear structure of tellurium isotopes [19,29,30] (including ^{129}Te) suggests that growth is caused rather by redistribution of transitions between low-lying nuclear levels connected with their microscopic nature.

V. CONCLUSIONS

The dependence of isomeric-yield ratios on bremsstrahlung endpoint energy has been measured for the reactions ^{120}Te$(\gamma,n)^{119}$Te^{m,g}, ^{122}Te$(\gamma,n)^{121}$Te^{m,g}, ^{124}Te$(\gamma,n)^{123}$Te^{m,g}, ^{128}Te$(\gamma,n)^{127}$Te^{m,g}, and ^{130}Te$(\gamma,n)^{129}$Te^{m,g} in the energy range 10–22 MeV. We obtained relatively high isomeric ratios for tellurium isotopes in spite of significant spin differences inside isomeric pairs. The values of isomeric ratios increase with the filling of the subshell $1h_{11/2}$ and are highest for ^{129}Te. It is notable that the observed effect of correlation between increasing possibility of isomers $J^\pi = 11/2^-$ excitation and growing of the neutrons number on subshell $1h_{11/2}$ cannot be associated with the contributions of statistical or pre-equilibrium mechanisms, but is rather a consequence the nonstatistical distribution of γ-ray transition probabilities resulting from peculiarities in level structure.

The cross sections of isomer population have been calculated with the inverse matrix method. Results were compared with TALYS-1.4 calculations. Theoretical calculations revealed the dominating role of the statistical model based on the Hauser-Feshbach formalism in the (γ,n) reactions and the contribution of the pre-equilibrium mechanism based on the exciton model is about 7% to 12%. In most cases, calculation reproduced the cross section and this can serve as evidence of the adequacy of statistical theory. But the case of the ^{130}Te$(\gamma,n)^{129}$Te^m reaction shows that results of calculations significantly depend on the properties of low-energy levels and transitions between them. Thus, without precise knowledge of nuclear structure, calculations of isomers excitation can produce misleading results.

ACKNOWLEDGMENTS

We are grateful to the Microtron M-30 and betatron B25/30 engineers for providing the beams during the experiment. We would also like to thank A. J. Koning for helpful discussions on TALYS calculations.

[1] V. D. Efros, W. Leidemann, G. Orlandini, and E. L. Tomusiak, Phys. Lett. B **484**, 223 (2000).

[2] R. Skibiński, J. Golak, H. Witala, W. Glöckle, H. Kamada, and A. Nogga, Phys. Rev. C **67**, 054002 (2003).

[3] A. V. Varlamov, V. V. Varlamov, D. S. Rudenko, and M. E. Stepanov, *Atlas of Giant Dipole Resonance* (IAEA, Vienna, 1999).

[4] V. M. Mazur, Phys. Part. Nuclei **31**, 188 (2000) (in Russian).

[5] Yu. P. Gangrsky and V. M. Mazur, Phys. Part. Nuclei **33**, 158 (2002) (in Russian).
[6] M. Arnauld and S. Goriely, Phys. Rep. **384**, 1 (2003).
[7] E. M. Burbidge, G. R. Burbidge, W. A. Fowler, and F. Hoyle, Rev. Mod. Phys. **29**, 547 (1957).
[8] D. L. Lambert, Astron. Astrophys. Rev. **3**, 201 (1992).
[9] C. Nair, A. R. Junghans, M. Erhard, D. Bemmerer, R. Beyer, E. Grosse, K. Kosev, M. Marta, G. Rusev, K. D. Schilling, R. Schwengner, and A. Wagner, Phys. Rev. C **81**, 055806 (2010).
[10] W. Hauser and H. Feshbach, Phys. Rev. **87**, 366 (1952).
[11] A. G. Belov, Yu. P. Gangrsky, A. P. Tonchev, and N. P. Balabanov, Phys. At. Nucl. **59**, 367 (1996) (in Russian).
[12] T. D. Thiep, T. T. An, P. V. Cuong, N. T. Khai, N. T. Vinh, A. G. Belov, and O. D. Maslov, J. Radioanal. Nucl. Chem. **289**, 637 (2011).
[13] A. J. Koning, S. Hilaire, and M. C. Duijvestijn, in *Proceedings of the International Conference on Nuclear Data for Science and Technology, Nice, France, April 22–27, 2007*, edited by O. Bersillon, F. Gunsing *et al*. (EDP Science, Les Ulis, 2008), pp. 211–214.
[14] S. P. Kapica and V. N. Melechin, *The Microtron* (Harwood Academic, London, 1978).
[15] D. M. Symochko, E. Browne, and J. K. Tuli, Nucl. Data Sheets **110**, 2945 (2009).
[16] S. Ohya, Nucl. Data Sheets **111**, 1619 (2010).
[17] S. Ohya, Nucl. Data Sheets **102**, 547 (2004).
[18] A. Hashizume, Nucl. Data Sheets **112**, 1647 (2011).
[19] Y. Tendow, Nucl. Data Sheets **77**, 631 (1996).
[20] R. Vänska and R. Rieppo, Nucl. Instrum. Methods **179**, 525 (1981).
[21] A. Lepretre, H. Beil, R. Bergere, P. Carlos, A. De Miniac, A. Veyssiere, and K. Kernbach, Nucl. Phys. A **219**, 39 (1974).
[22] O. V. Bogdankevich and F. A. Nikolaev, *Methods in Bremsstrahlung Research* (Academic Press, New York, 1996).
[23] A. J. Koning and M. C. Duijvestijn, Nucl. Phys. A **744**, 15 (2004).
[24] H. Gruppelaar, P. Nagel, and P. E. Hodgson, Nuovo Cimento **9**, 1 (1986).
[25] E. Gadioli and P. E. Hodgson, *Pre-equilibrium Nuclear Reaction* (Oxford University Press, Oxford, 1992).
[26] A. J. Koning and J. P. Delaroche, Nucl. Phys. A **713**, 231 (2003).
[27] P. Capote, M. Herman, and P. Oblozinsky, Nucl. Data Sheets **110**, 3107 (2009).
[28] W. Dilg, W. Schantl, H. Vonach, and M. Uhl, Nucl. Phys. A **217**, 269 (1973).
[29] H.-F. Wirth, T. von Egidy, I. Tomandl, J. Honzátko, D. Bucurescu, N. Marginean, V. Yu. Ponomarev, R. Hertenberger, Y. Eisermann, and G. Graw, Nucl. Phys. A **716**, 3 (2003).
[30] V. Bondarenko, J. Honzátko, I. Tomandl, D. Bucurescu, T. von Egidy, J. Ott, W. Schauer, H.-F. Wirth, and C. Doll, Phys. Rev. C **60**, 027302 (1999).
[31] J. Kopecky and M.U hl, Phys. Rev. C **41**, 1941 (1990).
[32] D. M. Brink, Nucl. Phys. **4**, 215 (1957).
[33] P. Axel, Phys. Rev. **126**, 671 (1973).
[34] M. A. M. Shahabuddin, J. A. Kuehner, and A. A. Pilt, Phys. Rev. C **23**, 64 (1981).
[35] H. Dias and L. Losano, Phys. Rev. C **50**, 1377 (1994).
[36] V. Bondarenko, J. Honzátko, and I. Tomandl, Z. Phys. A **354**, 235 (1996).